*J. Phys. Chem. A* **2004,** *108,* 2339−2345

# Theoretical Study of the Fast Photodissociation Channels of the Monohalobenzenes

**Ya-Jun Liu,[†] Petter Persson,[†,‡] and Sten Lunell*,[†]**

*Department of Quantum Chemistry, Uppsala University, Box 518, S-751 20 Uppsala, Sweden,*
*and Materials and Process Simulation Centre, Beckman Institute 13974,*
*California Institute of Technology, Pasadena, California 91125*

*Received: December 22, 2003; In Final Form: January 30, 2004*

Excited state properties of fluorobenzene, chlorobenzene, bromobenzene, and iodobenzene have been investigated theoretically using multireference CASSCF and CASPT2 methods. Experimentally, chlorobenzene and bromobenzene are known to exhibit one fast dissociation channel, whereas iodobenzene exhibits two fast dissociation channels. The calculations indicate that the chlorobenzene, the bromobenzene, and the slower iodobenzene dissociation channels are due to intersystem crossings from a bound ($\pi$,$\pi$*) singlet excited state to a repulsive (n,$\sigma$*) triplet excited state. The faster iodobenzene dissociation channel is instead found to be caused by a direct dissociation of an antibonding (n,$\sigma$*) singlet excited state. The CASPT2 calculations predict that the onset of fluorobenzene photodissociation should occur around 196 nm, with a single time constant longer than 1 ns. CASSCF geometries and accurate MSCASPT2 calculated vertical excitation energies are presented for the ground state as well as the first excited singlet and triplet states of all the monohalobenzenes.

## I. Introduction

Molecular photodissociation is a challenging area, and the results are imperative to decode the mechanism of many chemical reactions in atmospheric and biological chemistry.[1−5] The literature is rich with experimental and computational reports on the properties of the lowest triplet states and phosphoresence of aryl halides.[6−11] Their photodissociation processes and the properties of their excited states have also received attention from both experimental and theoretical studies. Photodissociation of iodobenzene (IBz) was studied using weak nanosecond lasers[12−23] and femtosecond pump−probe spectroscopy.[24] Density functional theory calculations[25] and spin−orbit (SO)-MCQDPT[26] calculations[27] have been used to study the excited states and dissociations of iodobenzene. Both experimental and theoretical studies revealed two reaction mechanisms of IBz: a direct dissociation caused by excitation to an antibonding (n,$\sigma$*) state and an indirect dissociation caused by a transition to a ($\pi$,$\pi$*) state of the phenyl ring that is predissociated by the (n,$\sigma$*) state. Photodissociation of bromobenzene (BrBz) has been extensively studied using photofragment translational spectroscopy (PTS),[28,29] femtosecond pump−probe spectroscopy,[24] and ultrafast transient absorption spectroscopy.[30] Hartree−Fock,[29] CASSCF,[30] and CASPT2[31] calculations were performed for the photodissociation of BrBz. There are also rich experimental reports about the photodissociation of chlorobenzene (ClBz),[24,28,32−35] but no high-level calculation about photodissociation of ClBz except some ab initio calculations on its low-lying triplet states.[11,36] These studies revealed that the photodissociation mechanism of BrBz and ClBz is due to intersystem crossing between a ($\pi$,$\pi$*) and a (n,$\sigma$*) state. We have not found any experimental or theoretical studies of the photodissociation of fluorobenzene (FBz) except its multiphoton ionization spectra.[37]

The main objective of this paper is to clearly interpret the fast photodissociation processes of IBz, BrBz, and ClBz observed by experiments, and to predict the nature of a possible fast photodissociation process of FBz. Providing theoretical information about both the ground state and a number of excited states for all the aryl halides, calculated at a consistently high level, significantly improves the possibilities to make reliable comparisons between the different molecules. For example, it may be possible to clarify to what extent observed differences in photodissociation rates are caused by subtle differences in the predissociation barriers of the excited states.

## II. Methodology and Computational Details

The geometries of the ground state, as well as the first singlet and triplet excited states of IBz, BrBz, ClBz, and FBz were optimized using the CASSCF method. Multireference CASSCF second-order perturbation theory[38,39] (MSCASPT2) was used to calculate the vertical excitation energies ($T_v$) of the three lowest singlet and triplet states of every irreducible representation. We determined the eight lowest singlet and the five lowest triplet states of IBz, the six lowest singlet and the five lowest triplet states of BrBz, the five lowest singlet and triplet states of ClBz, and the three lowest singlet and the four lowest triplet states of FBz. Ground and excited state potential energy curves (PEC) along the halogen−carbon bond distances of the aryl halides were calculated using the CASPT2 method. The phenyl geometries of the excited states were kept equal to the respective relaxed CASSCF optimized ground state geometry. The PECs of each molecule contain all the states that dissociate to ground state products, and some other states that dissociate to non ground state products. All these PECs were drawn adiabatically, and part of them were also drawn diabatically. In the CASSCF calculations, 12 electrons were active. Labeling the orbitals within the $C_{2v}$ point group in the order of $a_1$, $a_2$, $b_2$, and $b_1$, an active space denoted (2314) was used. The cc-pVDZ basis set[40] was used for C and H, and the relativistic ab initio model potential (AIMP) effective core potential (ECP) of Barandiaran

---

* Corresponding author. E-mail: Sten.Lunell@kvac.uu.se.
[†] Uppsala University.
[‡] California Institute of Technology.

10.1021/jp0379648 CCC: $27.50

**TABLE 1: CASSCF Ground State Geometries (Å) of the Aryl Halides**[a]

| | C−X[b] | $C_1$−$C_2$ | $C_2$−$C_3$ | $C_3$−$C_4$ |
|---|---|---|---|---|
| FBz[c] | 1.331 (1.327) | 1.395 (1.383) | 1.396 (1.395) | 1.388 (1.397) |
| ClBz[d] | 1.778 (1.741) | 1.392 (1.393) | 1.395 (1.396) | 1.387 (1.401) |
| BrBz[e] | 1.938 (1.879) | 1.392 (1.399) | 1.395 (1.397) | 1.387 (1.386) |
| IBz | 2.135 | 1.395 | 1.395 | 1.387 |

[a] The values in parentheses are experimental fitted structures. [b] X is F, Cl, Br, or I. [c] Experimental values from ref 43. [d] Experimental values from ref 44. [e] Experimental values from ref 45.

and Seijo[41] were used for I with 17 valence electrons, and Br, Cl, and F with 7 valence electrons. The states average technique was used in the CASSCF $T_v$ calculations. The 1s core of the carbon was frozen in the CASPT2 calculations. All the calculations were performed using the MOLCAS 5.4 quantum-chemistry software.[42] The same threshold and shift were used in all the CASPT2 calculations of singlet and triplet states.

## III. Results and Discussion

**A. Vertical Excitation Energies.** We used the CASSCF method to optimize the ground state geometries of FBz, ClBz, BrBz, and IBz. From Table 1, we can see that CASSCF optimized F−C (1.331 Å), Cl−C (1.778 Å), and Br−C (1.938 Å) bond distances are longer than the experimental fitted values[43−45] by 0.004, 0.037, and 0.059 Å, respectively, whereas the C−C bond distances agree very well with the corresponding experimental fitted values. We did not find any experimental fitted structure of IBz. Previous literature[11,27,29,30,32,36,45] has reported the optimized ground state geometry of FBz, ClBz, BrBz, or IBz by the HF, MP2, DFT, or CASSCF methods. As our main focus is on excited state properties, a detailed comparison with these results is not given here.

The MSCASPT2 method was used to calculate the vertical excitation energy, $T_v$, of the lowest singlet and triplet states of FBz, ClBz, BrBz, and IBz at their CASSCF optimized ground state geometries, respectively. From these calculations, we determined the three lowest singlet states of FBz to be $S_0$−$A_1$, $S_1$−$B_2$, and $S_2$−$A_1$, and the four lowest triplet states to be $T_1$−$A_1$, $T_2$−$A_1$, $T_3$−$B_2$, and $T_4$−$B_2$. All of them correspond to ($\pi$,$\pi$*) transitions; see Table 2. The five lowest singlet and the five lowest triplet states of ClBz were determined by the calculations to be $S_0$−$A_1$, $S_1$−$B_2$, $S_2$−$A_1$, $S_3$−$B_1$, and $S_4$−$B_2$ and $T_1$−$A_1$, $T_2$−$A_1$, $T_3$−$B_2$, $T_4$−$B_2$, and $T_5$−$B_1$, respectively. Except $S_3$ and $T_5$, which are ($\pi$,$\sigma$*) and (n,$\sigma$*) transitions, respectively, all the transitions have ($\pi$,$\pi$*) character; see Table 2. The six lowest singlet states and the five lowest triplet states of BrBz are $S_0$−$A_1$, $S_1$−$B_2$, $S_2$−$B_1$, $S_3$−$A_1$, $S_4$−$A_2$, and $S_5$−$B_2$ and $T_1$−$A_1$, $T_2$−$A_1$, $T_3$−$B_2$, $T_4$−$B_1$, and $T_5$−$B_2$, respectively. Except $S_2$ and $S_4$, which correspond to ($\pi$,$\sigma$*) transitions, and $T_4$, which is a (n,$\sigma$*) transition, all the excited states correspond to ($\pi$,$\pi$*) transitions; see Table 2. The eight lowest singlet states and the five lowest triplet states of IBz are $S_0$−$A_1$, $S_1$−$B_2$, $S_2$−$B_2$, $S_3$−$B_2$, $S_4$−$A_1$, $S_5$−$A_2$, $S_6$−$B_1$ and $S_7$−$A_2$ and $T_1$−$A_1$, $T_2$−$B_1$, $T_3$−$A_1$, $T_4$−$B_2$, and $T_5$−$B_2$, respectively. Among them, $S_1$, $S_3$, $S_6$, $T_2$, and $T_5$ correspond to (n,$\sigma$*) transitions, $S_2$, $S_4$, $T_1$, $T_3$, and $T_4$ correspond to ($\pi$,$\pi$*) transitions, $S_5$ is a ($\pi$,$\sigma$*) transition, and $S_7$ is a (n,$\pi$*) transition; see Table 2. All the $T_v$ values of the first singlet excited states of FBz, ClBz, BrBz, and IBz are near 4.6 eV. The first excited states of FBz, ClBz, and BrBz are all $B_2$ bound states. However, the first singlet excited state of IBz is a $B_1$ repulsive state (see section D for details). Interestingly, the $T_v$ difference between the $S_1$ and $S_2$ states of FBz, ClBz, BrBz, and IBz decreases systematically from 1.66 to 1.62, 0.89, and 0.1 eV, respectively; see Table 2.

**B. CASPT2 Calculated Potential Energy Curves.** To further clarify the photodissociation mechanisms, we calculated several CASPT2 PECs along the dissociation coordinate given by the $C_6H_5$-X (X is F, Cl, Br, or I) bond, for the lowest singlet and triplet states. In fact, many states dissociate to excited products, and most of them are not important for explaining the fast dissociation. Hence, we include all those curves that lead to ground state products, and only a few curves that lead to excited state products. The adiabatic PECs for FBz, ClBz, BrBz, and IBz, are shown in Figure 1a, Figure 2a, Figure 3a, and Figure 4a, respectively. The excited states have been labeled in increasing order of $T_v$ at the ground state minimum. To explain the phosphoresence and photodissociation of IBz, BrBz, and ClBz, we focus on the bound singlet and triplet states and those repulsive triplet states whose PEC lead to ground products. So, we extract these curves from Figures 1a, 2a, 3a, and 4a, respectively, and as far as possible, these curves are drawn diabatically so that they follow a particular electronic configuration through avoided crossings between two states of the same symmetry. This results in four simpler plots, Figures 1b, 2b, 3b, and 4b, for FBz, ClBz, BrBz, and IBz, respectively. Just as for the bromobenzenes,[31] there are always two singlet and three triplet excited states dissociating to the same energy limit as the ground state potential energy curve.

**C. Low-Lying Triplet States and Phosphoresence.** Because there are a lot of experimental and computational reports on the propertites of the lowest triplet states and phosphoresence of ClBz and BrBz,[6−11] we simply mention their transitions from triplet to ground states here. All the aryl halides have $C_{2v}$ symmetry, making the transitions from triplet $A_1$ and $B_2$ states to ground state $S_0$−$A_1$ allowed via spin−orbit coupling. Figures 2b, 3b, and 4b show that two bound ($\pi$,$\pi$*) triplet states, $T_1$−$A_1$ and $T_3$−$B_2$ for ClBz, $T_1$−$A_1$ and $T_3$−$B_2$ for BrBz, and $T_1$−$A_1$ and $T_4$−$B_2$ for IBz, were found below 4.66 eV (266 nm) in our calculations. $T_1$−$A_1$ and $T_3$−$B_2$ of ClBz are probably responsible for its dual phosphorescence observed by Takemura et al. in glassy matrixes.[7] The S → T absorption spectra of ClBz has its band maximum at 3.56 eV,[10] which is in good agrement with our predicted $T_v$ of 3.58 eV. It is worth mentioning that this CASPT2 calculated $T_v$ value is much better than the CASSCF calculated value (3.24 eV).[11] Again, $T_1$−$A_1$ and $T_3$−$B_2$ of BrBz are probably responsible for its dual phosphorescence observed by Okutsu et al. in glassy matrixes.[9] We did not find any experiments on the phosphorescence spectra of IBz and FBz. From the present calculations, the transitions from $T_1$−$A_1$ and $T_4$−$B_2$ to $S_0$−$A_1$ of IBz should also produce dual phosphorescence; see Figure 4b. However, Figure 1b shows that only one bound ($\pi$,$\pi$*) triplet state of FBz, $T_1$−$A_1$, was found below 4.66 eV (266 nm) in our calculations. From this we predict that there is just a single phosphorescence for FBz. To help understanding the transitions from triplet states to ground states, we also optimized the geometry of the first triplet state of FBz, ClBz, BrBz, and IBz; see Table 3.

**D. Photodissociations of the Low-Lying Excited States.** There are two basic types of photodissocition of a chemically bound molecule.[46] One is direct photodissociation, where a photon excites the molecule from the ground state to a higher repulsive electronic state, after which the excited complex fragments directly on a very short time scale. The other type is indirect photodissociation, of which there are two kinds. One is that a photon first excites a bound electronic state, which by itself cannot dissociate. However, if the molecule undergoes a transition from the bound state to another electronic state whose potential is repulsive, the complex will ultimately decay with a

**TABLE 2: CASPT2 Vertical Excitation Energies (eV) of the Lowest Singlet and Triplet Excited States of the Aryl Halides**[a]

| FBz | ClBz | BrBz | IBz |
|---|---|---|---|
| $S_0-A_1$ 0.00 | $S_0-A_1$ 0.00 | $S_0-A_1$ 0.00 | $S_0-A_1$ 0.00 |
| $S_1-B_2$ 4.74 ($\pi,\pi^*$) | $S_1-B_2$ 4.64 ($\pi,\pi^*$) | $S_1-B_2$ 4.74 ($\pi,\pi^*$) | $S_1-B_1$ 4.50 (n,$\sigma^*$) |
| $S_2-A_1$ 6.40 ($\pi,\pi^*$) | $S_2-A_1$ 6.26 ($\pi,\pi^*$) | $S_2-B_1$ 5.63 ($\pi,\sigma^*$) | $S_2-B_2$ 4.60 ($\pi,\pi^*$) |
| | $S_3-B_1$ 6.46 ($\pi,\sigma^*$) | $S_3-A1$ 6.13 ($\pi,\pi^*$) | $S_3-B_2$ 5.13 (n,$\sigma^*$) |
| | $S_4-B_2$ 6.83 ($\pi,\pi^*$) | $S_4-A_2$ 6.72 ($\pi,\sigma^*$) | $S_4-A_1$ 5.79 ($\pi,\pi^*$) |
| | | $S_5-B_2$ 6.73 ($\pi,\pi^*$) | $S_5-A_2$ 5.96 ($\pi,\sigma^*$) |
| | | | $S_6-B_1$ 6.45 (n,$\sigma^*$) |
| | | | $S_7-A_2$ 6.52 (n,$\pi^*$) |
| $T_1-A_1$ 3.75 ($\pi,\pi^*$) | $T_1-A_1$ 3.58 ($\pi,\pi^*$) | $T_1-A_1$ 3.63 ($\pi,\pi^*$) | $T_1-A_1$ 3.66 ($\pi,\pi^*$) |
| $T_2-A_1$ 4.52 ($\pi,\pi^*$) | $T_2-A_1$ 4.31 ($\pi,\pi^*$) | $T_2-A_1$ 4.35 ($\pi,\pi^*$) | $T_2-B_1$ 4.10 (n,$\sigma^*$) |
| $T_3-B_2$ 4.53 ($\pi,\pi^*$) | $T_3-B_2$ 4.48 ($\pi,\pi^*$) | $T_3-B_2$ 4.54 ($\pi,\pi^*$) | $T_3-A_1$ 4.34 ($\pi,\pi^*$) |
| $T_4-B_2$ 5.92 ($\pi,\pi^*$) | $T_4-B_2$ 5.61 ($\pi,\pi^*$) | $T_4-B_1$ 5.26 (n,$\sigma^*$) | $T_4-B_2$ 4.39 ($\pi,\pi^*$) |
| | $T_5-B_1$ 6.11 (n,$\sigma^*$) | $T_5-B_2$ 5.68 ($\pi,\pi^*$) | $T_5-B_2$ 4.57 (n,$\sigma^*$) |

[a] Transition classifications are given in parentheses.

rate that depends on the coupling between the two electronic states. The final fragmentation takes place in a different electronic state than the one originated excited by the photon. This process is called electronic predissociation or Herzberg's type I.[47] If the energy of the crossing point is so high that the excitation cannot reach the repulsive energy surface, no fast predissociation can take place. The other example is that the potential has a well at close distances and a barrier that blocks the dissociation channel. The barrier might be considered to be the result of an avoided crossing with a higher electronic state. In this case the photon excites quasi-stable (so-called "resonance") states inside the well which are prevented from immediate dissociation by the potential barrier. Such a state can decay either by tunneling through the barrier or by internal vibrational energy redistribution between the various nuclear degrees of freedom if more than two atoms are involved. The lifetime of the compound depends on the tunneling rate and (or) the efficiency of internal energy transfer. This process is called vibrational predissociation, or Herzberg's type II predissociation.[47]

In Figure 1b–4b, besides PECs of the bound triplet states mentioned above, the remaining curves are a bound singlet state $S_1-B_2$ and a repulsive triplet state $T_7-B_1$ for FBz, a bound singlet state $S_1-B_2$ and a repulsive triplet state $T_5-B_1$ for ClBz, a bound singlet state $S_1-B_2$ and a repulsive triplet state $T_4-B_1$ for BrBz, and a repulsive singlet state $S_1-B_1$, a bound singlet state $S_2-B_2$, and two repulsive triplet states, $T_2-B_1$ and $T_5-B_2$ for IBz.

We used CASSCF to optimize the geometries of the first singlet excited states of FBz, ClBz, and BrBz. The first singlet excited state of IBz is repulsive, so, we instead optimized the geometry of its second singlet excited state; see Table 3. We explain their photodissociation one by one in the following.

All experimental investigations of the photodissociation of BrBz at 266 nm have indicated decay via a single fast photodissociation channel.[24,29,30] Zhang et al.[29] first qualitatively proposed a fast predissociation induced by a coupling between a bound S state and a repulsive T state. Somewhat later, Rasmusson et al.[30] assigned this to the spin–orbit coupling between the bound $S_1-B_1$ state and the $T_3-B_2$ repulsive state (the apparent symmetric discrepancy between the present paper and ref 30 is due to different choices of coordinate systems). In ref 24, its time constant was measured to be 28 ps.

From our calculations, the Br–C bond distance of the $S_1-B_2$ state is 1.904 Å, which is 0.034 Å shorter than in the ground state; see Tables 1 and 3. From Figure 3b, the bound $S_1-B_2$ state, which is reached by a ($\pi,\pi^*$) transition, crosses a repulsive triplet state $T_4-B_1$, which is reached by a (n,$\sigma^*$) transition. The Br–C bond distance at the crossing point is about 1.96 Å. The $T_v$ value is about 4.91 eV at this point, which is near the 266 nm (4.66 eV) used in the experiments.[24,29,30] As errors in CASPT2 computed excitation energies are typically less than 0.3 eV,[48] we assign the dissociation with 28 ps lifetime[24] to a Herzberg's type I predissociation, with strong coupling between the bound $S_1-B_2$ state and the repulsive $T_4-B_1$ state leading to dissociation.

According to the present CASSCF calculations, the Cl–C bond distance of the $S_1-B_2$ state is 1.747 Å, which is 0.031 Å shorter than in its ground state; see Tables 1 and 3. The photodissociation situation of ClBz is similar to that of BrBz. The bound $S_1-B_2$ state, of ($\pi,\pi^*$) origin, crosses a repulsive $T_5-B_1$ state, of (n,$\sigma^*$) origin; see Figure 2b. The Cl–C bond distance at the crossing point is about 1.96 Å. The $T_v$ value at this point is about 5.15 eV, which is 0.49 eV higher than the 266 nm (4.66 eV) excitation energy used in the experiments.[24,32] This difference exceeds the anticipated CASPT2 calculation errors 0.3 eV. In fact, the crossed molecular beam technique did not detect such a fast photodissociation at 266 nm.[32] Freedman et al.[33] reported the photolysis of ClBz at 193 nm (6.42 eV), and Ichimura et al.[33] reported the photodecomposition of ClBz at 193 and 248 nm (5.00 eV). But the photodissociation studies using femtosecond pump–probe spectroscopy upon excitation at 266 nm detected a single time constant for ClBz with 1 ns.[24] Anyway, this fast dissociation is also an example of a Herzberg's type I predissociation, the strong coupling between the bound $S_1-B_2$ state and the replusive $T_5-B_1$ state being responsible for the dissociation.

The photodissociation of IBz is different from that of BrBz and ClBz. The experimental investigations using the velocity map imaging method,[25] state-selective one-dimensional translation spectroscopy[14,17] and femtosecond pump–probe spectroscopy[24] detected two time constants. The photodissociation studies using femtosecond pump–probe spectroscopy upon excitation at 266 nm gave two time constants for IBz with 700 and 350 fs.[24] El-Sayed and co-workers[14,16,20] as well as Zewail and co-workers[49] proposed that the faster dissociation is due to a direct dissociation of the repulsive triplet (n,$\sigma^*$) state, and the slower dissociation is due to a spin–orbit induced crossing from the triplet ($\pi,\pi^*$) state to the repulsive singlet (n,$\sigma^*$) state. Previous calculations using DFT and (SO)-MCQDPT methods[25,27] support this explanation. According to the present calculations, the first triplet excited state of IBz is not a repulsive state; see Figure 4b. However, the first singlet excited state, $S_1-B_1$, is a repulsive (n,$\sigma^*$) state with 4.5 eV $T_v$, which is 0.16 eV lower than 266 nm. So, the fast dissociation, 350 fs, was assigned to a direct dissociation resulting from excitation of

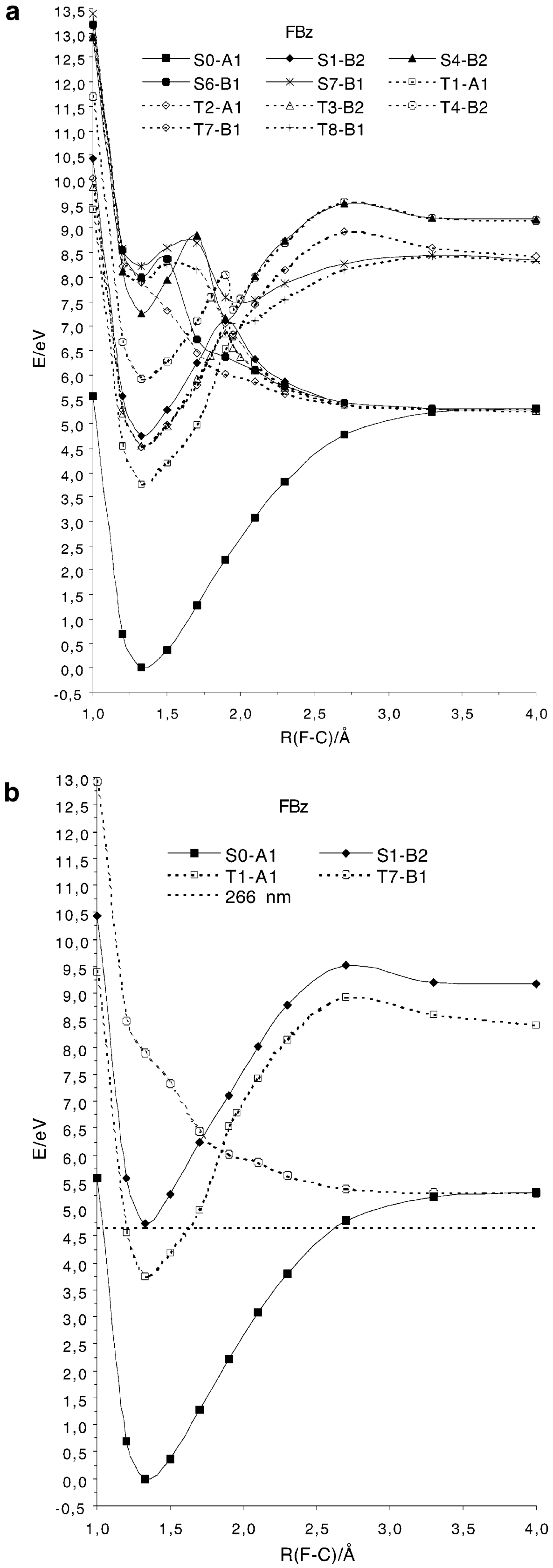

**Figure 1.** (a) CASPT2 adiabatic potential energy curves along the F−$C_6H_5$ bond distance of eleven states of fluorobenzene. The dashed lines are used for triplet states, and the solid lines are for singlet states. (b) CASPT2 diabatic potential energy curves along the F−$C_6H_5$ bond distance of four states of fluorobenzene. The dashed lines are used for triplet states, and the solid lines are used for singlet states. The horizontal dashed line indicates the 266 nm excitation energy, which has often been used in previous experiments.

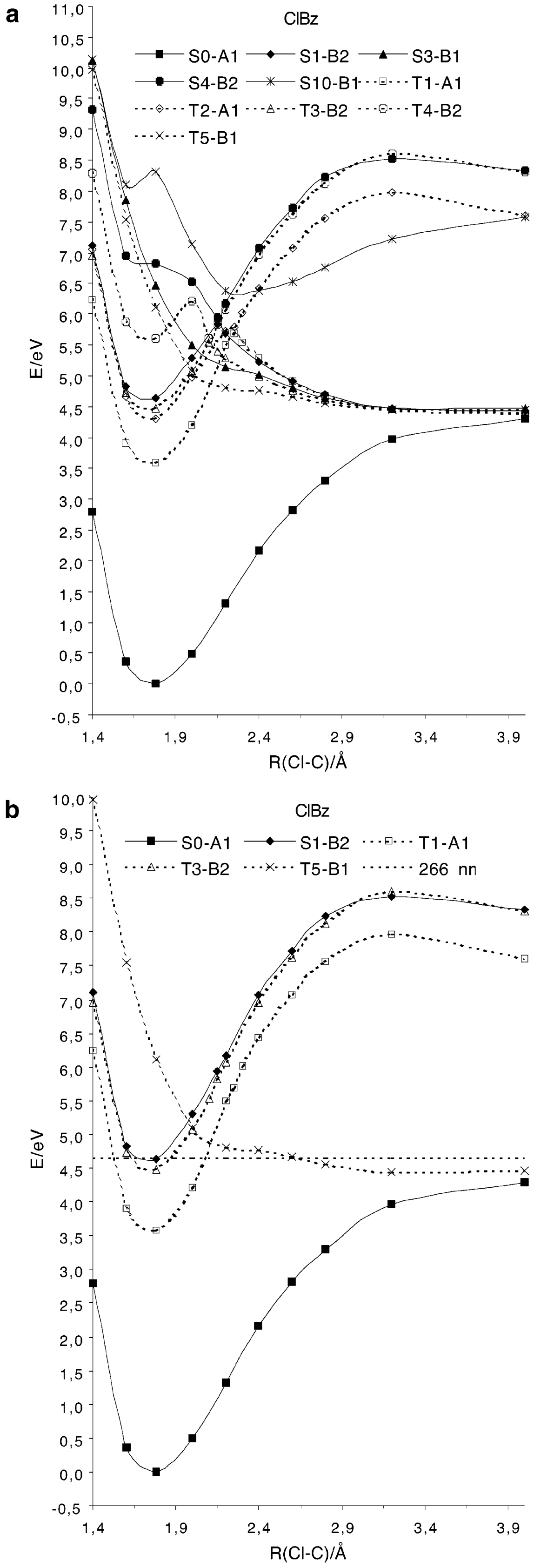

**Figure 2.** (a) CASPT2 adiabatic potential energy curves along the Cl−$C_6H_5$ bond distance of eleven states of chlorobenzene. The dashed lines are used for triplet states, and the solid lines are used for singlet states. (b) CASPT2 diabatic potential energy curves along the Cl−$C_6H_5$ bond distance of five states of chlorobenzene. The dashed lines are used for triplet states, and the solid lines are used for singlet states. The horizontal dashed line indicates the 266 nm excitation energy, which has often been used in previous experiments.

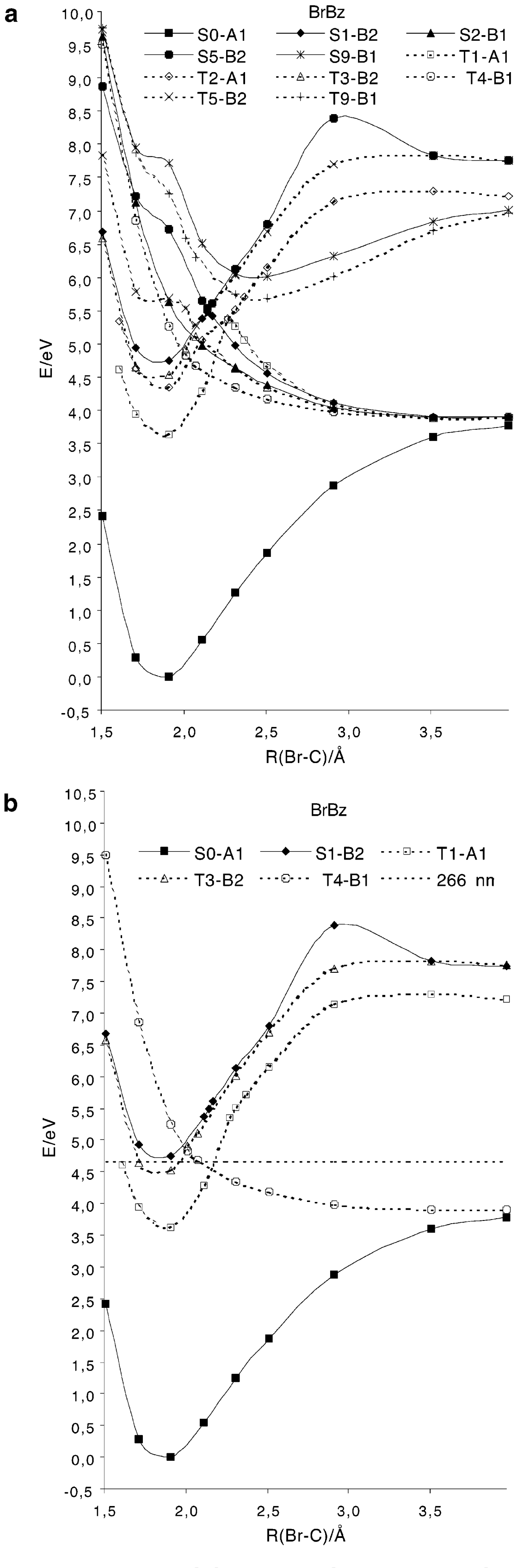

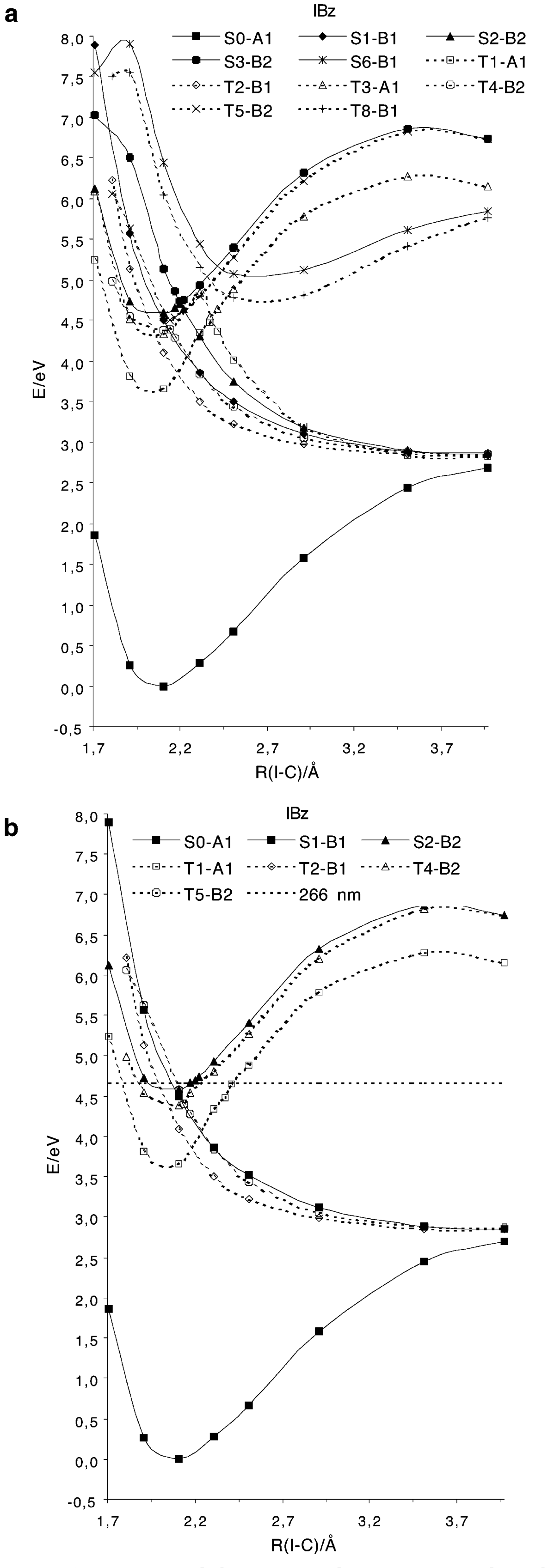

**Figure 3.** (a) CASPT2 adiabatic potential energy curves along the Br$-$C$_6$H$_5$ bond distance of eleven states of bromobenzene. The dashed lines are used for triplet states, and the solid lines are used for singlet states. (b) CASPT2 diabatic potential energy curves along the Br$-$C$_6$H$_5$ bond distance of five states of bromobenzene. The dashed lines are used for triplet states, and the solid lines are used for singlet states. The horizontal dashed line indicates the 266 nm excitation energy, which has often been used in previous experiments.

**Figure 4.** (a) CASPT2 adiabatic potential energy curves along the I$-$C$_6$H$_5$ bond distance of eleven states of iodobenzene. The dashed lines are used for triplet states, and the solid lines are used for singlet states. (b) CASPT2 diabatic potential energy curves along the I$-$C$_6$H$_5$ bond distance of seven states of iodobenzene. The dashed lines are used to triplet states, and the solid lines are used for singlet states. The horizontal dashed line indicates the 266 nm excitation energy, which has often been used in previous experiments.

**TABLE 3: CASSCF Geometries (Å) of the First Singlet and Triplet Excited States of the Aryl Halides**[a]

| | FBz | | ClBz | | BrBz | | IBz | |
|---|---|---|---|---|---|---|---|---|
| | $S_1-B_2$ | $T_1-A_1$ | $S_1-B_2$ | $T_1-A_1$ | $S_1-B_2$ | $T_1-A_1$ | $S_2-B_2$ | $T_1-A_1$ |
| $C-X$[b] | 1.320 | 1.331 | 1.747 | 1.775 | 1.904 | 1.936 | 2.094 | 2.098 |
| $C_1-C_2$ | 1.395 | 1.393 | 1.456 | 1.392 | 1.455 | 1.391 | 1.459 | 1.476 |
| $C_2-C_3$ | 1.434 | 1.513 | 1.438 | 1.513 | 1.439 | 1.514 | 1.439 | 1.338 |
| $C_3-C_4$ | 1.458 | 1.377 | 1.394 | 1.376 | 1.394 | 1.376 | 1.393 | 1.468 |

[a] The first singlet excited state of IBz is repulsive state. [b] X is F, Cl, Br, or I.

**TABLE 4: CASPT2 $T_v$ Values at the Crossing Points between the Singlet $(\pi,\pi^*)$ State and the Triplet Repulsive $(n,\sigma^*)$ State and the Time Constants for the Aryl Halides**

| | $T_v$ (eV) | lifetime (ps)[a] |
|---|---|---|
| FBz | 6.33 | |
| ClBz | 5.15 | 1000 |
| BrBz | 4.91 | 28 |
| IBz[b] | 4.33 | 0.7 |

[a] From ref 24. [b] There are two triplet repulsive states, $T_2-B_1$ and $T_5-B_2$, that cross the bound $S_2-B_1$ state of IBz; see Figure 4b. The $T_v$ value of the second crossing point is 4.50 eV.

$S_1-B_1$. The first bound singlet excited state of IBz is a $S_2-B_2$ state with a $T_v$ of 4.60 eV. The I−C bond distance of the $S_2-B_2$ state is 2.094 Å, which is 0.041 Å shorter than that of its ground state; see Tables 1 and 3. From Figure 4b, the bound $S_2-B_2$ state $(\pi,\pi^*)$, crosses two repulsive triplet excited states, $T_2-B_2$ and $T_5-B_2$, at points where the I−C bond is about 1.96 and 2.10 Å, respectively. Both $T_2-B_2$ and $T_5-B_2$ are $(n,\sigma^*)$ states, the $T_v$ values of the two crossing points being 4.33 and 4.50 eV, respectively. These energies are both lower than the 266 nm excitation used in the experiment.[24] So, in agreement with earlier calculations,[25,27] we assign another fast photodissociation, 700 fs, to a Herzberg type I predissociation, with the strong couplings between the bound $S_2-B_2$ state and the repulsive $T_2-B_2$ and $T_5-B_2$ states leading to dissociation. It is worth mentioning that the crossing point between the $S_2-B_2$ and $T_2-B_2$ states is very low in energy, and close to the minimum of this $S_2-B_2$ state; see Figure 4b. It is therefore conceivable that this process becomes a direct dissociation.

To our knowledge, there is no available experimental or theoretical photodissociation study of FBz to date. From our calculations, the F−C bond distance of the $S_1-B_2$ state is 1.320 Å, which is close to that of its ground state, 1.331 Å; see Tables 1 and 3. From Figure 1b, the bound $S_1-B_2$ $(\pi,\pi^*)$ state, crosses a repulsive triplet $T_7-B_1$ $(n,\sigma^*)$ state. The F−C bond distance at the crossing point is about 1.74 Å, and the $T_v$ value at this point is about 6.33 eV.

The time constants for the decay of the initially bound excited $(\pi,\pi^*)$ states are 700 fs for IBz, 28 ps for BrBz, and 1 ns for ClBz.[24] Obviously, the dissociation times increase with decreasing atomic number of the halogen, because the spin−orbit coupling between the singlet $(\pi,\pi^*)$ state and the triplet repulsive $(n,\sigma^*)$ state is strongly enhanced by the presence of heavy substituents. From the present calculations, the $T_v$ values of the crossing points between the singlet $(\pi,\pi^*)$ state and the triplet repulsive $(n,\sigma^*)$ state are 4.33, 4.91, 5.15, and 6.33 eV for IBz, BrBz, ClBz, and FBz, respectively. Table 4 gives these barriers and the corresponding lifetime of the aryl halides. The difference between the X−C bond distance of the ground state and the first bound singlet state is 0.041, 0.034, 0.031, and 0.011 Å for IBz, BrBz, ClBz, and FBz, respectively. Thus, both the $T_v$ values at the crossing points and the differences of X−C bond distances increase with decreasing halogen atomic number. From the above analysis, we predict that the fast photodissociation of FBz should take place above 6.33 eV, which is 196 nm, and its time constant should be longer than 1 ns.

Comparing the potential energy surfaces of the four aryl halides reveals several trends that help to explain their photoexcitation and photodissociation behavior. The similarity in photoexcitation energy for excitations to the first excited singlet states of all the aryl halides is a result of the presence, in each case, of a ring $\pi-\pi^*$ excitation to a bound excited singlet state. This excitation is affected very little by the halogen, and therefore the shapes of the potential energy curves of the first bound excited singlet states are also very similar to the corresponding ground state potential energy curves, only displaced upward in energy.

In contrast, the photodissociation properties are strikingly different for the four aryl halides, with increasingly fast photodissociation on progression down the halogen series. In addition to the heavy atom effect increasing the spin−orbit coupling with increasing halogen mass, this may in part be explained by a systematic shift of the minima of the first bound excited singlet states toward the repulsive states. A comparison among Figures 1b−4b shows that the first bound excited state minima shift upward in energy relative to the ground state dissociation limit, and outward in carbon−halogen bond distance, as the halogen gets heavier. This is, in turn, a result of the similarity of this state with the ground state, noted above, which displays exactly this behavior due to the increasing halogen radius associated with increasing atomic number. The repulsive states, on the other hand, have the same dissociation limit as the corresponding ground states, and are therefore not shifted to the same extent in the interstate crossing region. As a result, the predissociation barrier is large for fluorobenzene, becomes successively smaller for chlorobenzene and bromobenzene, and is virtually nonexistent for iodobenzene.

## IV. Conclusions

To explain the fast dissociation of chlorobenzene and bromobenzene, and the two fast dissociations for iodobenzene, observed by experiments, as well as predict the fast photodissociation behavior of fluorobenzene, we calculated CASPT2 potential energy curves of their singlet and triplet states. The fast dissociations of chlorobenzene and bromobenzene, and the somewhat less fast dissociation of iodobenzene are assigned to Herzberg's type I predissociation. These dissociations are due to intersystem crossings between the initially excited bound $(\pi,\pi^*)$ singlet state and a repulsive $(n,\sigma^*)$ triplet excited state. For bromobenzene, strong spin−orbit coupling occurs between the bound $S_1-B_2$ state and the repulsive $T_4-B_1$ state. For chlorobenzene, strong spin−orbit coupling occurs between the bound $S_1-B_2$ state and the repulsive $T_5-B_1$ state. However, for iodobenzene, strong spin−orbit couplings instead take place between the bound $S_2-B_2$ state and two repulsive states, $T_2-B_2$ and $T_5-B_2$. The faster of the two fast dissociations of iodobenzene is due to direct dissociation of the $S_1-B_1$ state, which is an antibonding $(n,\sigma^*)$ state. The present CASPT2 calculations predict that there should be a fast photodissociation process of fluorobenzene, which has not been reported by experiment, at about 196 nm with a single time constant longer than 1 ns. Moreover, this paper also reported accurate MSCASPT2 calculated vertical excitation energies for the whole homologous series of monohalobenzenes, and the CASSCF calculated geometries of their ground state, the first singlet and triplet excited states.

**Acknowledgment.** The Swedish Research Council (VR), the Swedish Supercomputer Center (NSC), and the Magnus Bergvall Foundation are gratefully acknowledged for their support.

## References and Notes

(1) Riley, S. J.; Wilson, K. R. *Faraday Discuss. Chem. Soc.* **1972**, *53*, 132.

(2) Dzvonik, M.; Yang, S.; Bersohn, R. *J. Chem. Phys.* **1974**, *61*, 4408.

(3) Leone, S. R. *Adv. Chem. Phys.* (Dynamics of the excited state), L, **1983**, 255.

(4) Houston, P. *Annu. Rev. Phys. Chem.* **1989**, *40*, 375.

(5) Bersohn, R. In *Molecular Photodissociation Dynamics*; Ashfold, M. N. R., Baggott, J. E., Eds.; Royal Society of Chemistry: London, 1987.

(6) Ichimura, T. Hikida, T.; Mori, Y. *J. Phys. Chem.* **1975**, *79*, 291.

(7) Takemura, T.; Yamada, Y.; Baba, H. *Chem. Phys.* **1982**, *68*, 171.

(8) Takemura, T.; Yamada, Y.; Sugawara, M.; Baba, H. *J. Phys. Chem.* **1986**, *90*, 2324.

(9) Okutsu, T.; Kageyama, T.; Kounose, N.; Tsuchiya, J.; Hiratsuka, H. *Chem. Phys. Lett.* **1999**, *299*, 597.

(10) Mcglynn, S. P.; Azumi, T.; Kinoshita, M. *Molecular Spectroscopy of triplet state*; Prentice Hall: Engelwood Cliffs, NJ, 1969.

(11) Rubio-Pons, O.; Loboda, O.; Minaev, B.; Schimmelpfenning, B.; Vahtras, O.; Ågren, H. *Mol. Phys.* **2003**, *101*, 2103.

(12) Kavita, K.; Das, P. K. *J. Chem. Phys.* **2002**, *117*, 2038.

(13) Freedman, A.; Yang, S. C.; Kawasaki, M.; Bersohn, R. *J. Chem. Phys.* **1980**, *72*, 1028.

(14) Hwang, H. J.; El-Sayed, M. A. *J. Photochem. Photobiol. A* **1996**, *102*, 13.

(15) Hwang, H. J.; El-Sayed, M. A. *J. Chem. Phys.* **1991**, *94*, 4877.

(16) Hwang, H. J.; El-Sayed, M. A. *J. Phys. Chem.* **1992**, *96*, 8728.

(17) Griffiths, J. A.; Jung, K. W.; El-Sayed, M. A. *J. Phys. Chem.* **1996**, *100*, 7989.

(18) Frietas, J. E.; Hwang, H. J.; El-Sayed, M. A. *J. Phys. Chem.* **1995**, *99*, 7395.

(19) Hwang, H. J.; Griffiths, J. A.; El-Sayed, M. A. *Int. J. Mass Spectrom. Ion Processes* **1994**, *131*, 265.

(20) Frietas, J. E.; Hwang, H. J.; El-Sayed, M. A. *J. Phys. Chem.* **1994**, *98*, 3322.

(21) Dietz, T. D.; Duncan, M. A.; Liverman, M. G.; Smalley, R. E. *J. Chem. Phys.* **1980**, *73*, 4816.

(22) Pence, W. H.; Baughcum, S. L.; Leone, S. R. *J. Phys. Chem.* **1981**, *85*, 3844.

(23) Doering, J. P. *J. Chem. Phys.* **1977**, *67*, 4065; **1969**, *51*, 2866.

(24) Kadi, M.; Davidsson, J.; Tarnovsky, A. N.; Rasmusson, M.; Åkesson, E. *Chem. Phys. Lett.* **2001**, *350*, 93.

(25) Unny, S.; Du, Y.; Zhu, L.; Truhins, K.; Robert, K.; Sugita, A.; Kawasaki, M.; Matsumi, Y.; Delmdahl, R.; Parker, D. H.; Berces, A. *J. Phys. Chem. A* **2001**, *105*, 2270.

(26) Fedorov, D. G.; Finley, J. P. *Phys. Rev. A* **2001**, *64*, 042502.

(27) Ajitha, D.; Fedorov, D. G.; Finley, J. P.; Hirao, K. *J. Chem. Phys.* **2002**, *117*, 7068.

(28) Park, M. S.; Lee, K. W.; Jung, K.-H. *J. Chem. Phys.* **2001**, *114*, 10368.

(29) Zhang, H.; Zhu, R.-S.; Wang, G.-J.; Han, K.-L.; He, G.-Z.; Lou, N.-Q. *J. Chem. Phys.* **1999**, *110*, 2922.

(30) Rasmusson, M.; Lindh, R.; Lascoux, N.; Tarnovsky, A. N.; Kadi, M.; Kuhn, O.; Sundström, V.; Åkesson, E. *Chem. Phys. Lett.* **2003**, *367*, 759.

(31) Liu, Y.-J.; Persson, P.; Karlsson, H. O.; Lunell, S.; Kadi, M.; Karlsson, D.; Davidsson, J. *J. Chem. Phys.*, in press.

(32) Wang, G.-J.; Zhu, R.-S.; Zhang, H.; Han, K.-L.; He, G.-Z.; Lou, N.-Q. *Chem. Phys. Lett.* **1998**, *288*, 429.

(33) Freedman, A.; Yang, S. C.; Kawasaki, M.; Bersohn, R. *J. Chem. Phys.* **1980**, *72*, 1028.

(34) Ichimura, T.; Mori, Y.; Shinohara, H.; Nishi, N. *Chem. Phys.* **1994**, *189*, 117.

(35) Ichimura, T.; Mori, Y. *J. Chem. Phys.* **1973**, *58*, 288.

(36) Nagaoka, S.; Takeshi, T.; Baba, H.; Koga, N.; Morokuma, K. *J. Phys. Chem.* **1986**, *90*, 759.

(37) Murakami, J.; Kaya, K.; Ito, M. *J. Chem. Phys.* **1980**, *72*, 3263.

(38) Andersson, K.; Malmqvist, P.-Å.; Roos, B. O. *J. Chem. Phys.* **1992**, *96*, 1218.

(39) Finley, J.; Malmqvist, P.-Å.; Roos, B. O.; Serrano-Andrés, L. *Chem. Phys. Lett.* **1998**, *288*, 299.

(40) Woon, D. E.; Dunning, T. H. *J. Chem. Phys.* **1993**, *98*, 1358.

(41) Barandiaran, Z.; Sijo, L. *Can. J. Chem.* **1992**, *70*, 409.

(42) Andersson, K.; Fulscher, M. P.; Lindh, R.; Malmqvist, P.-Å.; Olsen, J.; Sadlej, A. J.; Widmark, P.-O. MOLCAS version 5.4; University of Lund: Lund, Sweden, 2000.

(43) Doraiswamy, S.; Sharma, S. D. *J. Mol. Struct.* **1983**, *102*, 81.

(44) Cradock, S.; Muir, J. M.; Rankin, D. W. H. *J. Mol. Struct.* **1990**, *220*, 205.

(45) Peebles, S. A.; Peebles, R. A. *J. Mol. Struct.* **2003**, *107*, 657.

(46) Schinke, R. *Photodissociation Dynamics*; Cambridge University Press: Cambridge, U.K., 1993.

(47) Herzberg, G. *Molecular Spectra and Molecular Structure III. Spectra of Polyatomic Molecules*; Van Nostrand: New York, 1967.

(48) Merchan, M.; Serrano-Andres, L.; Fülscher, M. P.; Roos, B. O. In *Recent Advances in Multireference Theory*; Hiro, K. (University of Tokyo), Ed.; World Scientific: Singapore, 1999; Vol. IV, pp 161−196.

(49) Cheng, P. Y.; Zhong, D.; Zewail, A. H. *Chem. Phys. Lett.* **1995**, *237*, 399.